ChemComm

Chemical Communications

www.rsc.org/chemcomm

Volume 48 | Number 26 | 28 March 2012 | Pages 3141–3248

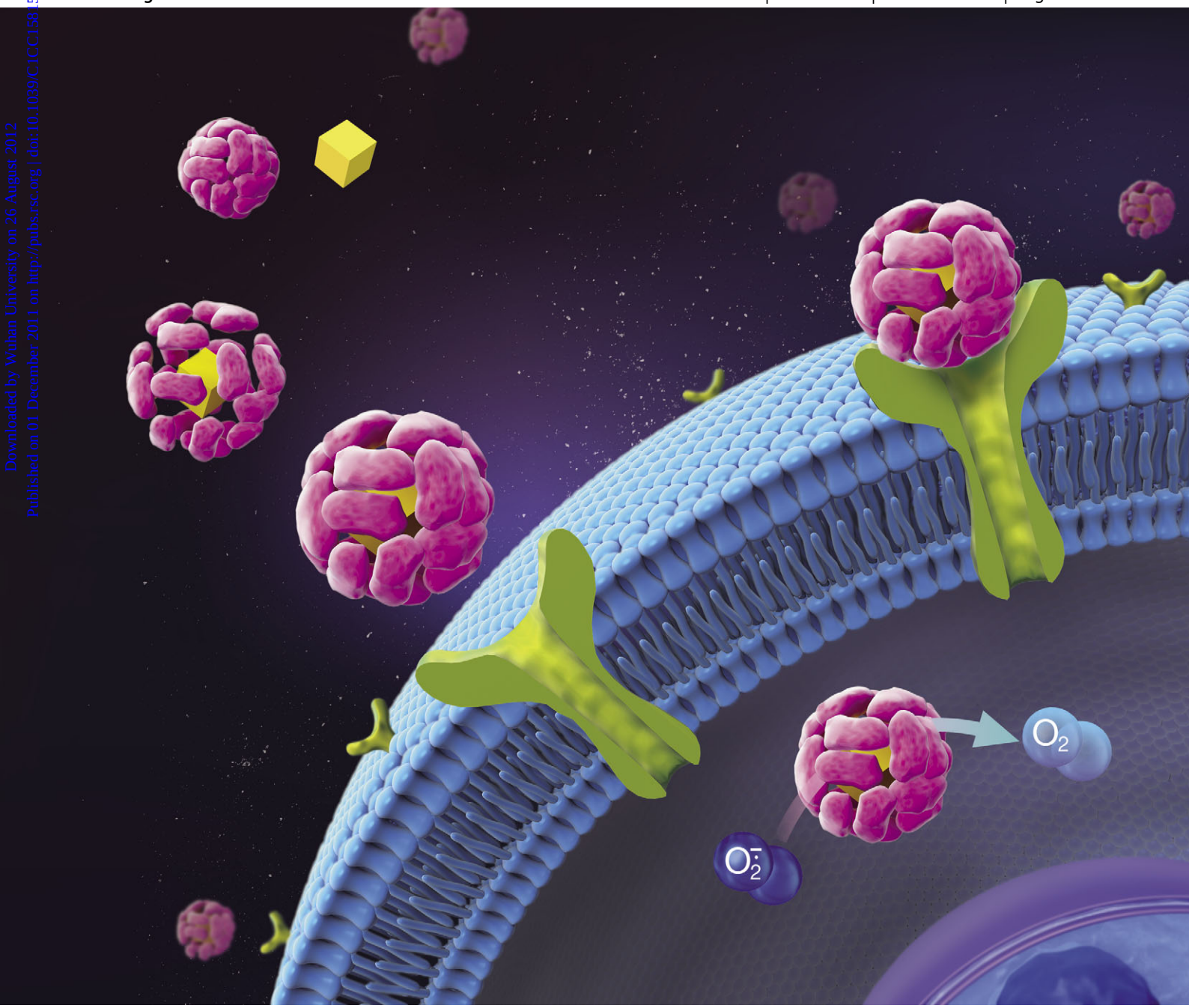

ISSN 1359-7345

RSC Publishing

COMMUNICATION

Ding Ma *et al.*

Apoferritin–CeO_2 nano-truffle that has excellent artificial redox enzyme activity

1359-7345(2012)48:26;1-8

ChemComm

Dynamic Article Links
View Online

Cite this: *Chem. Commun.*, 2012, **48**, 3155–3157

www.rsc.org/chemcomm

COMMUNICATION

Apoferritin–CeO_2 nano-truffle that has excellent artificial redox enzyme activity†

Xiangyou Liu,‡[ab] Wei Wei,‡[c] Quan Yuan,[a] Xin Zhang,[d] Ning Li,[e] Yuguang Du,[b] Guanghui Ma,[c] Chunhua Yan[a] and Ding Ma*[a]

Received 20th September 2011, Accepted 1st November 2011
DOI: 10.1039/c1cc15815e

4.5 nm nanoceria particles are successfully encapsulated into the apoferritin cavity *via* a dissociation–reconstruction route. The apoferritin coating not only improves the biocompatibility and changes the cellular uptake route of nanoceria, but also manipulates the electron localization at the surface of the nanoparticle thereby ameliorating the ROS-scavenging activity.

Incomplete removal of reactive oxygen species (ROS), which cause oxidative damage to human beings, leads to various detrimental effects on human health.[1] Natural antioxidant enzymes including endogenous superoxide dismutase (SOD)[2] may not be sufficient to protect cells from sudden oxidative damage. There is therefore intense interest in developing an active artificial enzyme with a high ROS-scavenging activity but low cytotoxicity. Some nanomaterials were reported to be able to act as antioxidants,[3,4] among which nanoceria particles (nano-CeO_2) drew much more attention due to their SOD mimetic activity and their reversibility and auto-regenerative properties.[5–7] However, it is still a challenge to construct a highly active artificial enzyme (even more active than SOD) with outstanding biocompatibility. Here we have shown that reconstructing a cage protein, apoferritin, to encapsulate the 4.5 nm nano-CeO_2 could fulfill this goal. Apoferritin not only improved the biocompatibility of the nano-CeO_2, but also manipulated the electron localization at the surface of the nanoparticle thereby ameliorating the ROS-scavenging activity of the apoferritin–CeO_2 hybrid nanocomposite (AFt–CeO_2).

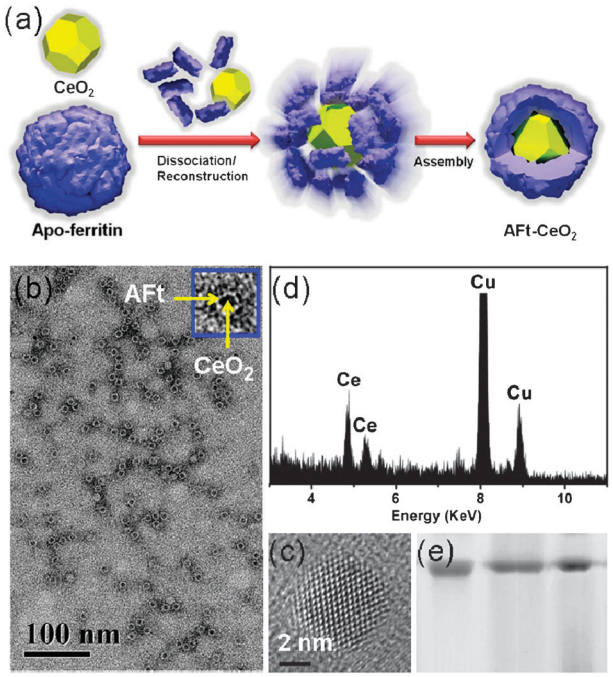

Fig. 1 (a) Schematic presentation of the assemblage process of AFt–CeO_2. (b) TEM image of negatively stained AFt–CeO_2. The inset shows an enlarged single AFt–CeO_2 nanocomposite. (c) HRTEM image of a single AFt–CeO_2 nanoparticle. (d) Energy dispersive spectrum of AFt–CeO_2. The signal of Cu is from the Cu grid. (e) Native PAGE gel of ferritin, AFt–CeO_2 and apoferritin (AFt) (from left to right).

The cage protein, apoferritin (the soft shell), was reconstructed into the nano-complex with the nano-CeO_2 (the hard core) wrapped into the central cavity of apoferritin *via* a dissociation–reconstruction process (Fig. 1a).[8,9] To the best of our knowledge, the nano-CeO_2, with all the faces being the most chemically active (100) facet and a narrow size distribution centered around 4.5 nm (Fig. S1, ESI†), have not been synthesized before. A transmission electron microscopy (TEM) image of negatively stained AFt–CeO_2 showed that all the nano-crystals were encapsulated inside the apoferritin cage (Fig. 1b). These discrete nano-crystals were further proved to be nano-CeO_2 by high-resolution TEM (HRTEM) (Fig. 1c) and energy dispersive spectroscopic measurements (Fig. 1d). Circular dichroism (CD) spectra revealed no

[a] *Beijing National Laboratory for Molecular Sciences, College of Chemistry and Molecular Engineering, Peking University, Beijing 100871, China. E-mail: dma@pku.edu.cn; Fax: +86-10-62758603; Tel: +86-10-62758603*
[b] *Dalian Institute of Chemical Physics, Chinese Academy of Sciences, Dalian 116023, China*
[c] *National Key Laboratory of Biochemical Engineering, Institute of Process Engineering, Chinese Academy of Sciences, Beijing 100190, China*
[d] *Department of Molecular and Experimental Medicine, The Scripps Research Institute, 10550 North Torrey Pines Road, La Jolla, CA 92037, USA*
[e] *Lab of Applied Biocatalysis, South China University of Technology, Guangzhou 510640, China*

† Electronic supplementary information (ESI) available: Experimental details and supplementary results. See DOI: 10.1039/c1cc15815e

‡ These authors contributed equally to this work.

significant changes in the secondary structure of apoferritin after the encapsulation of nanoceria (Fig. S2, ESI†). The integrality of AFt–CeO_2 was further validated by native polyacrylamide gel electrophoresis (PAGE) analysis which showed identical mobilities for ferritin, apoferritin, and AFt–CeO_2 (Fig. 1e). Inductively coupled plasma optical emission spectrometry (ICP-OES) analysis of the protein bands in Fig. 1e showed that cerium was detected in the band of AFt–CeO_2 but not in the other two bands. Taken together, these results confirmed the successful reconstitution of apoferritin in which nano-CeO_2 were integrated.

We then asked whether AFt–CeO_2 would possess an altered ROS-scavenging activity. To this end, we measured the ability of AFt–CeO_2 to quench ROS and compared its activity to other materials including natural SOD. Notably, AFt–CeO_2 was able to clear more than 70% of superoxide anions ($O_2^{\bullet -}$), while the natural SOD could only quench ~20% at most (Fig. 2a and b). Apoferritin-encapsulated Pt nanoparticles (AFt–Pt) were also able to quench superoxide anions,[10] however, the efficiency of AFt–Pt in ROS scavenging was much lower than that of AFt–CeO_2. As shown in Fig. S3 (ESI†) and Fig. 2a, the IC50 of AFt–Pt (56 μM) was more than 160 fold higher than that of the AFt–CeO_2 (0.34 μM).§ Interestingly, nano-CeO_2, AFt alone or the mixture of these two materials did not possess the same ROS-scavenging activity as AFt–CeO_2. At fixed cerium and protein concentrations, pristine nano-CeO_2 and apoferritin could quench less than ~10% of superoxide anions, while the direct mixture of nano-CeO_2 and apoferritin (AFt + CeO_2) merely quenched no more than 15% of superoxide anions (Fig. 2b). These observations directly demonstrated that the bio-conjugation of nano-CeO_2 with apoferritin conferred a superb ROS scavenging activity.

Why did the AFt–CeO_2 prove to be such a highly efficient artificial redox enzyme? It has been suggested that the reactivity of ceria in a redox process is largely dependent on the surface defects or vacancies on the crystals.[11] We then reasoned that the apoferritin modification improved the reducing activity of the nano-CeO_2. To test this hypothesis, electron energy loss spectroscopy (EELS) analysis was used to characterize the chemical state of nano-CeO_2 with and without an apoferritin corona (Fig. 2c). EELS in the M-edge region of cerium carries information on the initial state 4f occupancy. The spectra were characterized by sharp white lines of $3d_{3/2} \rightarrow 4f_{5/2}$ (M_4) and $3d_{5/2} \rightarrow 4f_{7/2}$ (M_5) associated with spin–orbit splitting. The relative intensities of the white lines were associated with the 4f-shell occupancy of cerium, and thus could be used to determine its valence states.[12] A method for calculating the valence state of Ce can be found in ref. 12. The result of this calculation was that pristine nano-CeO_2 had a 100% content of Ce^{4+} while the AFt–CeO_2 was a mixture of Ce^{3+} and Ce^{4+}, with an estimated 70% fraction of Ce^{3+}. This fact strongly indicated the existence of a charge transfer at the interface of the protein corona and the nano-CeO_2, resulting in a valence change of the oxide (Fig. S4, ESI†). A similar valence change has also been observed in the process where native ferritin sequesters and releases iron in the living biological systems, during which the valency of Fe oscillates between +2 and +3.[13,14] The charge transfer process changed the localization of electrons on the surface of nano-CeO_2 inside the apoferritin, and more importantly, induced the formation of surface defects and vacancies on the nano-CeO_2.[15] It is well-established that more defects or vacancies on the surface result in a much higher redox activity,[7,16] which explains the superior reactivity of AFt–CeO_2 in the ROS-scavenging assay.

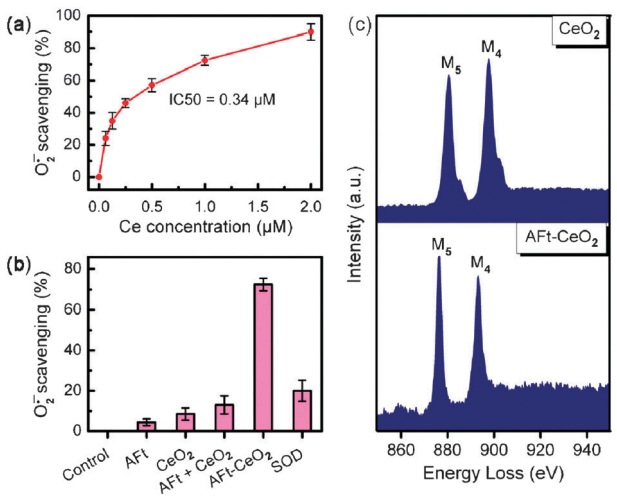

Fig. 2 (a) Dose-dependent $O_2^{\bullet -}$ scavenging by AFt–CeO_2. (b) Comparison of $O_2^{\bullet -}$ scavenging activity. The protein concentrations of AFt, AFt–CeO_2, "AFt + CeO_2" and SOD are all 0.01 μM, while the cerium concentrations of CeO_2, AFt–CeO_2 and "AFt + CeO_2" are 1 μM. (c) EELS profiles of pristine nano-CeO_2 and AFt–CeO_2.

The superb ROS-scavenging activity of AFt–CeO_2 made it a promising candidate to serve as an artificial redox enzyme to relieve the oxidative stress of living cells. To test its activity in living cells, we used a ROS-sensitive fluorescent dye, DCFH-DA (2,7-dichlorofluorescein diacetate), which could be oxidized to a highly fluorescent compound DCF by intracellular ROS.[17] HepG2 cells were preincubated with either nano-CeO_2 or AFt–CeO_2 before they were subjected to H_2O_2 treatment. Subsequently, the fluorescent level of DCF was used as an indicator of the residual ROS level. From several independent experiments, AFt–CeO_2 was convincingly shown to scavenge intracellular ROS more efficiently than nano-CeO_2 (Fig. 3a). Quantitatively, the IC50 of AFt–CeO_2 was 6.8 μM, ~20 times lower than that of nano-CeO_2 (132.2 μM). This result was further confirmed by corresponding images of confocal laser scanning microscopy (CLSM) (Fig. 3b). In the absence of nano-CeO_2 and AFt–CeO_2, the cells were strongly fluorescent, indicating a high ROS level. However, the fluorescent signal of AFt–CeO_2-pretreated HepG2 cells was significantly diminished, suggesting an efficiently reduced ROS level. Notably, HepG2 cells pretreated with nano-CeO_2 still exhibited a significant level of fluorescent intensity, indicating a rather limited reducing activity of nano-CeO_2 (Fig. 3b).

To test whether cells adapted readily to AFt–CeO_2 treatment, we examined the cellular internalization and cytotoxicity of AFt–CeO_2. As shown in Fig. 4a, the amount of internalized AFt–CeO_2 in HepG2 cells was about 2 fold higher than that of nano-CeO_2, implying that the AFt–CeO_2 was preferentially taken by HepG2 cells. Both CLSM and TEM images also confirmed that more AFt–CeO_2 nanocomplexes could be internalized in HepG2 cells than nano-CeO_2 (Fig. 4b–e). Interestingly, although AFt–CeO_2 entered HepG2 cells efficiently, cells were still viable in the presence of a high concentration of

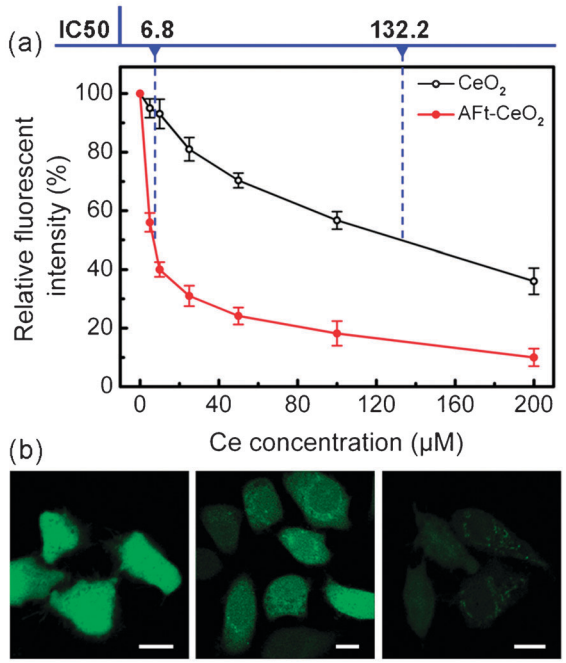

Fig. 3 (a) Scavenging of ROS by AFt–CeO_2 and nano-CeO_2 in HepG2 cells. (b) Representative CLSM images of H_2O_2-treated HepG2 cells after staining with DCFH-DA. From left to right: control, cells preincubated with nano-CeO_2 (25 μM) and AFt–CeO_2 (25 μM). All the scale bars represent 10 μm.

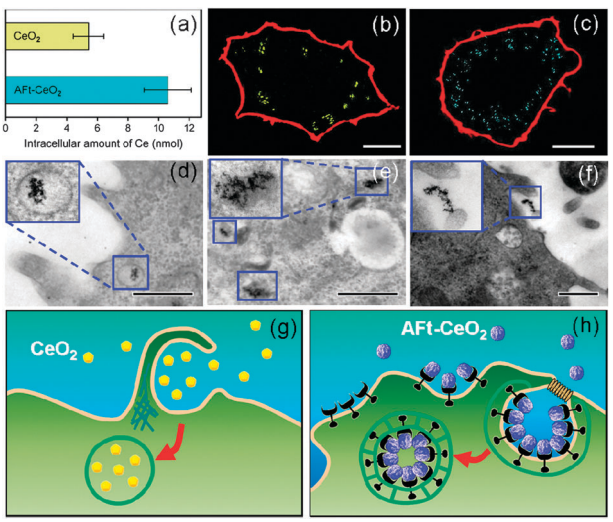

Fig. 4 (a) Quantification of AFt–CeO_2 and nano-CeO_2 internalized by HepG2 cells. (b–e) Representative CLSM and TEM images of HepG2 cells with nano-CeO_2 (b, d) or AFt–CeO_2 (c, e) internalized. In CLSM images (b) and (c), the bright spots in the cytoplasm around the nuclei are the internalized nano-CeO_2 (b) or AFt–CeO_2 (c) particles. (f) TEM image showing the typical macropinocytosis movement for nano-CeO_2 particles to enter HepG2 cells. (g and h) Schematic illustration of the macropinocytosis for nano-CeO_2 and the clathrin-mediated endocytosis for AFt–CeO_2. The scale bars in (b) and (c) represent 10 μm, while those in (d–f) represent 500 nm.

AFt–CeO_2 (Fig. S5, ESI†). How did cells adapt to the AFt–CeO_2 with a high internalized amount and a low cytotoxicity? We speculated that this distinct feature of AFt–CeO_2 was partially attributed to the apoferritin corona, which could potentially promote the cellular internalization process mediated *via* specific ferritin receptors and prevent the adverse interactions between the nano-CeO_2 and biomolecules in the cytoplasm.[18] Further study (Fig. S6, ESI†) also suggested that the internalization of AFt–CeO_2 was primarily regulated by clathrin-mediated endocytosis (Fig. 4h), while the internalization of the nano-CeO_2 was a macropinocytosis process (Fig. 4f and g).

In conclusion, we have demonstrated a strategy, combining cage proteins with a novel synthetic nano-material, to construct a novel nano-complex (AFt–CeO_2) that has proven to be by far the most active artificial redox enzyme with mimetic SOD activity. The modification of the surface of nano-CeO_2 has changed the intrinsic properties of individual building blocks, conferring a superb redox activity to the AFt–CeO_2. In addition, the cage proteins carry their biological identities to the AFt–CeO_2 to initiate an endocytosis process and improve its biocompatibility. This is a step-forward for the rational design/construction of artificial enzymes with designated functions, which have the potential to treat incurable diseases like some types of amyotrophic lateral sclerosis due to the failure of defense against ROS.

Acknowledgements. This work received financial support from the Natural Science Foundation of China (20603036, 21073004). The authors gratefully thank Miss Hua Yue and Mr. Zhanguo Yue for their help.

Notes and references

§ All the concentrations of AFt–CeO_2 mentioned in this study are the concentrations of Ce, unless otherwise stated.

1 J. Nordberg and E. S. J. Arnér, *Free Radical Biol. Med.*, 2001, **31**, 1287–1312.
2 J. M. Matés, *Toxicology*, 2000, **153**, 83–104.
3 M. Kajita, K. Hikosaka, M. Iitsuka, A. Kanayama, N. Toshima and Y. Miyamoto, *Free Radical Res.*, 2007, **41**, 615–626.
4 A. S. Karakoti, S. Singh, A. Kumar, M. Malinska, S. Kuchibhatla, K. Wozniak, W. T. Self and S. Seal, *J. Am. Chem. Soc.*, 2009, **131**, 14144–14145.
5 C. Korsvik, S. Patil, S. Seal and W. T. Self, *Chem. Commun.*, 2007, 1056–1058.
6 A. S. Karakoti, N. A. Monteiro-Riviere, R. Aggarwal, J. P. Davis, R. J. Narayan, W. T. Self, J. McGinnis and S. Seal, *JOM*, 2008, **60**, 33–37.
7 E. G. Heckert, A. S. Karakoti, S. Seal and W. T. Self, *Biomaterials*, 2008, **29**, 2705–2709.
8 B. Hennequin, L. Turyanska, T. Ben, A. M. Beltrán, S. I. Molina, M. Li, S. Mann, A. Patanè and N. R. Thomas, *Adv. Mater.*, 2008, **20**, 3592–3596.
9 E. Valero, S. Tambalo, P. Marzola, M. Ortega-Muñoz, F. J. López-Jaramillo, F. Santoyo-González, J. D. López, J. J. Delgado, J. J. Calvino, R. Cuesta, J. M. Domínguez-Vera and N. Gálvez, *J. Am. Chem. Soc.*, 2011, **133**, 4889–4895.
10 L. B. Zhang, L. Laug, W. Münchgesang, E. Pippel, U. Gösele, M. Brandsch and M. Knez, *Nano Lett.*, 2010, **10**, 219–223.
11 F. Esch, S. Fabris, L. Zhou, T. Montini, C. Africh, P. Fornasiero, G. Comelli and R. Rosei, *Science*, 2005, **309**, 752–755.
12 L. J. Wu, H. J. Wiesmann, A. R. Moodenbaugh, R. F. Klie, Y. M. Zhu, D. O. Welch and M. Suenaga, *Phys. Rev. B*, 2004, **69**, 9.
13 M. T. F. Telling and S. H. Kilcoyne, *Phys. B*, 2006, **374–375**, 451–455.
14 F. Bou-Abdallah, *Biochim. Biophys. Acta, Gen. Subj.*, 2010, **1800**, 719–731.
15 P. Dutta, S. Pal, M. S. Seehra, Y. Shi, E. M. Eyring and R. D. Ernst, *Chem. Mater.*, 2006, **18**, 5144–5146.
16 E. Mamontov, T. Egami, R. Brezny, M. Koranne and S. Tyagi, *J. Phys. Chem. B*, 2000, **104**, 11110–11116.
17 C. P. Lebel, H. Ischiropoulos and S. C. Bondy, *Chem. Res. Toxicol.*, 1992, **5**, 227–231.
18 X. Y. Liu, W. Wei, C. L. Wang, H. Yue, D. Ma, C. Zhu, G. H. Ma and Y. G. Du, *J. Mater. Chem.*, 2011, **21**, 7105–7110.